

Primljen / Received: 7.8.2020.

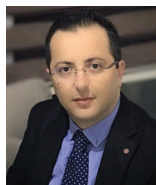
Ispravljen / Corrected: 24.2.2021.

Prihvaćen / Accepted: 10.5.2021.

Dostupno online / Available online: 10.8.2021.

# Structural health monitoring of beams with moving oscillator: theory and laboratory

## Authors:



Assist.Prof. **Reza Goldaran**, PhD. CE  
Girne American University, Girne, N. Cyprus  
Faculty of Engineering  
Civil Engineering Department  
[rezagoldaran@gmail.com](mailto:rezagoldaran@gmail.com)



Assist.Prof. **Mehdi Kouhdaragh**, PhD. CE  
Islamic Azad University, Malekan, Iran  
Civil Engineering Department, Malekan Branch  
[mehdikouhdaragh@gmail.com](mailto:mehdikouhdaragh@gmail.com)  
**Corresponding author**

Research Paper

**Reza Goldaran, Mehdi Kouhdaragh**

## Structural health monitoring of beams with moving oscillator: theory and laboratory

In this paper, a new intelligent portable mechanical system is introduced experimentally and theoretically to detect damage employing the fuzzy-genetic algorithm and EMD. For this purpose, the acceleration-time history is obtained from three points of a simply-supported beam utilizing accelerometer sensors. The gained signal is decomposed into small components by using an EMD method. Each decomposed component contains a specific frequency range. Finally, the proposed algorithm is designed to find the location and severity of damage through the frequency variation pattern among the safe and the damaged beam.

### Key words:

damage detection, vibration generating system, empirical mode decomposition, signal processing, fuzzy-genetic algorithm

Prethodno priopćenje

**Reza Goldaran, Mehdi Kouhdaragh**

## Praćenje stanja greda pomoću pomičnog oscilatora: teorija i eksperiment

U ovom se radu daje eksperimentalni i teoretski prikaz novog inteligentnog prenosivog mehaničkog sustava za otkrivanje oštećenja u kojem se koristi neizraziti genetski algoritam i metoda empirijskog rastavljanja (EMD). Za te je potrebe akcelerometrima izmjereno ubrzanje u vremenu na tri točke proste grede. Dobiveni signal rastavljen je metodom EMD na male komponente. Svaka komponenta sadrži određeni raspon frekvencija. Na kraju je provedeno projektiranje predloženog algoritma kako bi se utvrdilo mjesto i razina oštećenja na temelju obrasca variranja frekvencija na neoštećenoj i oštećenoj gredi.

### Ključne riječi:

otkrivanje oštećenja, sustav za generiranje vibracija, empirijsko rastavljanje, obrada signala, neizraziti genetski algoritam

## 1. Introduction

Defects and failures in structures, which are detrimental of human life and financial resources, can be eliminated through structural damage identification methods that have been studied previously through the literature. Among these methods, modal analysis methods are very popular due to practicality. These methods are based on the fact that modal parameters (natural frequency, mode shape, and modal damping) depend on the physical parameters (mass, damping, stiffness) and therefore any changes in physical parameters can lead to a change in modal parameters of the structure [1-2]. Typically, primary data for the comparison can be derived from the measured data of the intact structure or the finite element model. The modal parameters used to identify structural defects include frequency function, natural frequencies, mode shape curvature, modal bending, and so forth [3-6]. Any damage detection system is divided into several sections such as damage identification, identification of damage location, damage rate detection, and prediction of the damaging lifetime. In order to obtain an efficient performance, the presence of a very precise mathematical modelling of the monitored systems is vital. Modelling errors can affect performance of damage detection systems, especially in nonlinear monitored systems. The use of computational intelligence methods may compensate the modelling errors to provide a good approximation of nonlinear systems. Lia Ding et al. at Western Australian University evaluated the dynamic vehicle axle loads on bridges with different surface conditions. The innovation of this study was the application of the "evolutionary spectral method" to assess dynamic loads of the vehicles on the beam moving on a rough surface of the beam at constant velocity [6]. Jean-Charles et al. at the Civil Engineering department of the University of Tokyo proposed a method for prediction of vehicle-induced local responses and application to a skewed girder bridge [7]. Law et al. worked on identification of the vehicle axle load on the bridge deck at the Hong Kong Polytechnic School of Engineering. The axial loads applied to the beam were estimated based on an irregular road surface profile [8]. Neves et al. at the University of Porto used a direct method for analysing the vertical vehicle-structure interaction. Their proposed method is more suitable for systems with high structural volume than those that are constantly updated [9]. Law et al. studied the statistical prediction of the dynamic response of a beam structure with uncertain properties due to random passage of moving loads. The uncertain properties of the beam structure were assumed to be Gaussian and were modelled using the finite element method. The uncertain properties of the vehicle with Gaussian distribution were presented using the Karhunen-Loève Expansion. Na et al. used the Genetic Algorithm (GA) to detect stiffness changes in a twenty-story shear frame [11]. Marano et al. used the GA method to detect damage in a shear frame with incomplete measurements [12]. Mosquera et al. used GA to detect displacement changes on a two-span bridge in El

Centro [13]. Loh et al. modelled a three-dimensional crack in a structure and used wavelet and Fourier transforms to identify damage in an RC frame employing a shake table test [14]. Ganguli et al. presented the damage as stiffness reduction in modulus of elasticity and detected the location and the severity of damage on a helicopter blade by using a fuzzy logic system [15]. Among modal parameters, natural frequency is the most commonly used since it can be easily and accurately measured. In the present study, a new intelligent portable mechanical system is proposed for damage detection in beam-shaped structures using the fuzzy-genetic algorithm. The advantages of this technique are as follows:

- It could be applied for the mixed type of structures due to the system's simplicity and efficiency.
- The EMD (*Empirical Mode Decomposition*) method and Short-time Fourier Transform are utilized to extract natural frequency, which is different from previous works.

The current technique is able to identify the location and severity of damage in diverse modes. In this paper, a moving load including a concentrated mass and a linear elastic spring with constant velocity is used to excite a simply-supported beam dynamically. The acceleration-time history is extracted from three points of the beam by using the accelerometer sensors. To convert the acceleration-time history into usable information for damage identification, the EMD method is utilized. In this manuscript, the empirical method of signal decomposition into the main modes is firstly introduced and the capabilities of the method for damage detection are investigated. Then the signal components known as intrinsic mode functions (IMFs) gained by the EMD method are converted to the frequency range using the short-time Fourier transform method. The dominant frequencies of each IMF are used as features of the Fuzzy-Genetic Algorithm (FGA) to detect the location and severity of damage in the structure.

## 2. Modelling beam vibration system and moving oscillator

### 2.1. Equation of motion of moving oscillator

Figure 1 shows a moving oscillator that is a half-oscillator model with 4 degree of freedom with the constant speed  $v$  on a simply supported beam. The free diagram of moving oscillator for Figure 1 is shown in Figure 2. The four degree of freedom of this moving oscillator include:

- The vertical motion  $y_1$  of the unsprung mass  $m_1$
- The vertical motion  $y_2$  of the unsprung mass  $m_2$
- The vertical motion  $y_v$  of the sprung mass  $m_v$  that is known as the vertical movement
- Angular momentum  $\theta_v$  of the sprung mass

This is the vibration system of the basic activation function that is provided by  $y_3$  and  $y_4$  displacements. All displacements

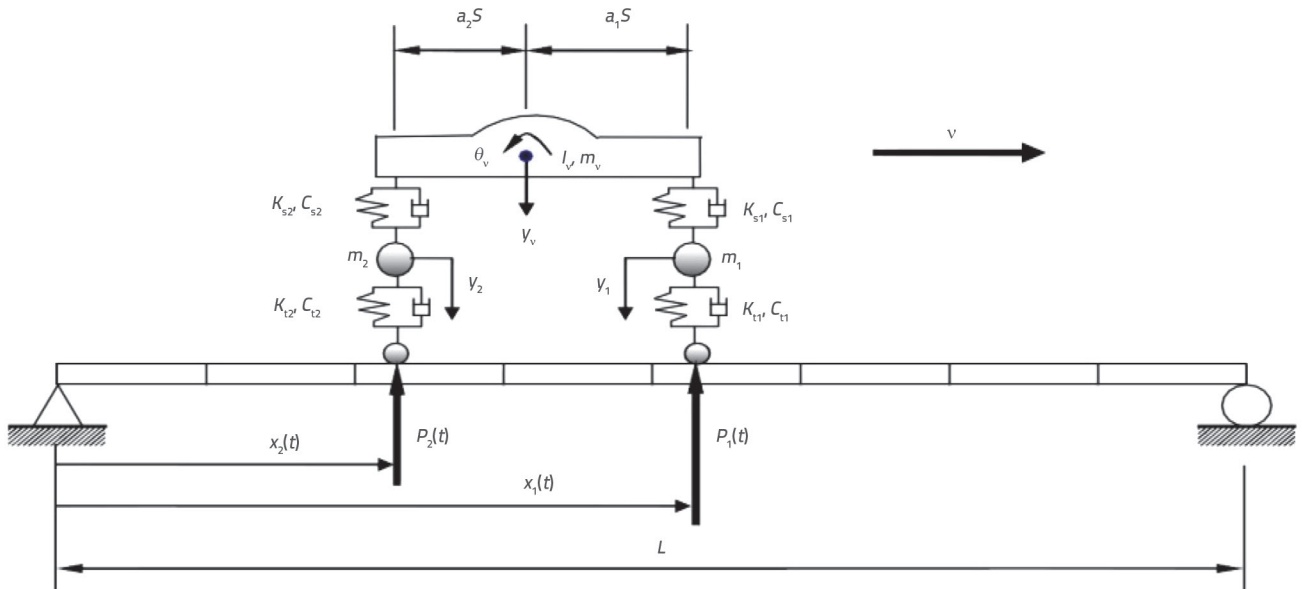


Figure 1. Coupled beam-moving oscillator system

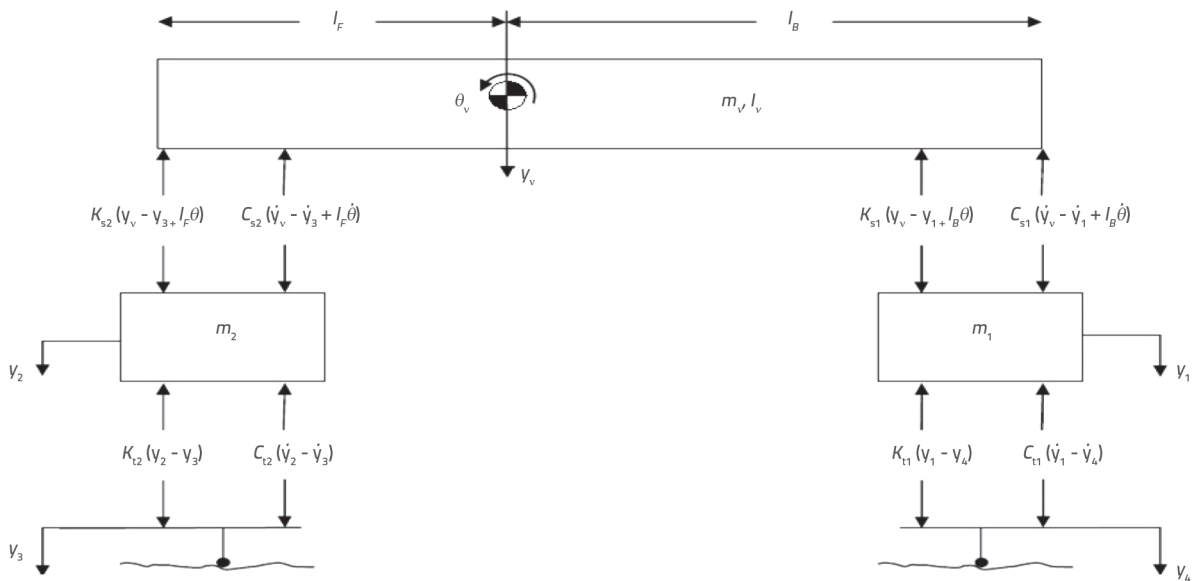


Figure 2. Free diagram of moving oscillator

are measured against their static situation, and  $\theta_v$  is considered to be small. The equations of motion of every four degree of freedom of the moving oscillator are modeled using Newton's second law, which is obtained as follows after simplification:

$$\begin{bmatrix} m_v & 0 & 0 & 0 \\ 0 & I_v & 0 & 0 \\ 0 & 0 & m_1 & 0 \\ 0 & 0 & 0 & m_2 \end{bmatrix} \begin{bmatrix} \ddot{y}_v \\ \ddot{\theta}_v \\ \ddot{y}_1 \\ \ddot{y}_2 \end{bmatrix} + \begin{bmatrix} C_{s1} + C_{s2} & I_F C_{s2} - I_B C_{s1} & -C_{s1} & -C_{s2} \\ I_F C_{s2} - I_B C_{s1} & I_B^2 C_{s1} + I_F^2 C_{s2} & I_B C_{s1} & -I_F C_{s2} \\ -C_{s1} & I_B C_{s1} & C_{s1} + C_{t1} & 0 \\ -C_{s2} & -I_F C_{s2} & 0 & C_{s2} + C_{t2} \end{bmatrix} \begin{bmatrix} \dot{y}_v \\ \dot{\theta}_v \\ \dot{y}_1 \\ \dot{y}_2 \end{bmatrix} + \begin{bmatrix} K_{s1} + K_{s2} & I_F K_{s2} - I_B K_{s1} & -K_{s1} & -K_{s2} \\ I_F K_{s2} - I_B K_{s1} & I_B^2 K_{s1} + I_F^2 K_{s2} & I_B K_{s1} & -I_F K_{s2} \\ -K_{s1} & I_B K_{s1} & K_{s1} + K_{t1} & 0 \\ -K_{s2} & -I_F K_{s2} & 0 & K_{s2} + K_{t2} \end{bmatrix} \begin{bmatrix} y_v \\ \theta_v \\ y_1 \\ y_2 \end{bmatrix} = \begin{bmatrix} 0 \\ 0 \\ (C_{t1})\dot{y}_4 + (K_{t1})y_4 \\ (C_{t2})\dot{y}_3 + (K_{t2})y_3 \end{bmatrix} \quad (1)$$

Because  $y_3$  and  $y_4$  values are not known,  $P(t)$  matrix can be defined as follows:

$$P(t) = \begin{bmatrix} (C_{t1})\dot{y}_4 + (K_{t1})y_4 \\ (C_{t2})\dot{y}_3 + (K_{t2})y_3 \end{bmatrix} = \begin{bmatrix} P_1(t) \\ P_2(t) \end{bmatrix} =$$

$$\begin{bmatrix} (m_1 + a_2 m_v)g + K_{t1} (y_1 - w(\hat{x}_1(t), t) - r(\hat{x}_1(t))) + C_{t1} (\dot{y}_1 - \dot{w}(\hat{x}_1(t), t)) \\ (m_2 + a_1 m_v)g + K_{t2} (y_2 - w(\hat{x}_2(t), t) - r(\hat{x}_2(t))) + C_{t2} (\dot{y}_2 - \dot{w}(\hat{x}_2(t), t)) \end{bmatrix} \quad (2)$$

Accordingly,  $P(t)$  is obtained from the sum total of static forces resulting from the moving oscillator and of the forces resulting from the beam-moving oscillator interaction.

In Equation (2),  $r(x)$  is the surface roughness of the beam at the point  $x$ ,  $\hat{x}_1(t)$  and  $\hat{x}_2(t)$  are the location of front and back axes of the moving oscillator, respectively, at the time  $t$ ;  $g$  denotes the acceleration of gravity;  $w(\hat{x}_1(t), t)$  and  $w(\hat{x}_2(t), t)$  are the

vertical deflection of beam body at the points where the front and back forces are exerted, respectively, at the time  $t$ . Point  $(.)$  indicates the time derivative. The following notations are made to simplify the forms of equations of motion:

$$\begin{aligned}
 M_{V1} &= \begin{bmatrix} m_v & 0 \\ 0 & I_v \end{bmatrix}; M_{V2} = \begin{bmatrix} m_1 & 0 \\ 0 & m_2 \end{bmatrix}; C_{V11} = \begin{bmatrix} C_{s1} + C_{s2} & I_f C_{s2} - I_b C_{s1} \\ I_f C_{s2} - I_b C_{s1} & I_b^2 C_{s1} + I_f^2 C_{s2} \end{bmatrix}; C_{V12} = \begin{bmatrix} -C_{s1} & -C_{s2} \\ I_b C_{s1} & -I_f C_{s2} \end{bmatrix}; \\
 C_{V21} &= \begin{bmatrix} -C_{s1} & I_b C_{s1} \\ -C_{s2} & -I_f C_{s2} \end{bmatrix}; C_{V22} = \begin{bmatrix} C_{s1} + C_{t1} & 0 \\ 0 & C_{s2} + C_{t2} \end{bmatrix}; K_{V11} = \begin{bmatrix} K_{s1} + K_{s2} & I_f K_{s2} - I_b K_{s1} \\ I_f K_{s2} - I_b K_{s1} & I_b^2 K_{s1} + I_f^2 K_{s2} \end{bmatrix}; \\
 K_{V12} &= \begin{bmatrix} -K_{s1} & -K_{s2} \\ I_b K_{s1} & -I_f K_{s2} \end{bmatrix}; K_{V21} = \begin{bmatrix} -K_{s1} & I_b K_{s1} \\ -K_{s2} & -I_f K_{s2} \end{bmatrix}; K_{V22} = \begin{bmatrix} K_{s1} + K_{t1} & 0 \\ 0 & K_{s2} + K_{t2} \end{bmatrix}; C_t = \\
 \begin{bmatrix} C_{t1} & 0 \\ 0 & C_{t2} \end{bmatrix}; K_t &= \begin{bmatrix} K_{t1} & 0 \\ 0 & K_{t2} \end{bmatrix}; P_0 = \begin{pmatrix} (m_1 + a_2 m_v)g \\ (m_2 + a_1 m_v)g \end{pmatrix}; Y = \begin{bmatrix} y_v \\ 0 \\ y_1 \\ y_2 \end{bmatrix};
 \end{aligned} \tag{3}$$

Thus, Equation (3) may be rewritten as Equation (4) that is the equation of motion of the moving oscillator.

$$\begin{bmatrix} M_{V1} & 0 \\ 0 & M_{V2} \end{bmatrix} \ddot{Y} + \begin{bmatrix} C_{V11} & C_{V12} \\ C_{V21} & C_{V22} \end{bmatrix} \dot{Y} + \begin{bmatrix} K_{V11} & K_{V12} \\ K_{V21} & K_{V22} \end{bmatrix} Y = \begin{bmatrix} 0 \\ P(t) \end{bmatrix} \tag{4}$$

### 2.2. Equation of beam

Mass and stiffness matrices of beam elements are derived using the Hermit splines shape functions. The result for each element can be expressed as follows, Equations (5) and (6):

$$K_t = \frac{2EI}{l^3} \begin{bmatrix} 6 & 3l & -6 & 3l \\ 3l & 2l^2 & -3l & l^2 \\ -6 & -3l & 6 & -3l \\ 3l & l^2 & -3l & 2l^2 \end{bmatrix} \tag{5}$$

$$M_t = \frac{\rho l A}{420} \begin{bmatrix} 156 & 22l & 54 & -13l \\ 22l & 4l^2 & 13l & -3l^2 \\ 54 & 13l & 156 & -22l \\ -13l & -3l^2 & -22l & 4l^2 \end{bmatrix} \tag{6}$$

By integrating matrices for each element in a general matrix, the mass matrix and stiffness of the entire structure have been achieved. By considering the Rayleigh damping for beam and boundary conditions, the equation of the vibrating beam can be written as:

$$M_b \ddot{R} + C_b \dot{R} + K_b R = H_b P \tag{7}$$

In Equation (7),  $M_b$ ,  $C_b$  and  $K_b$  are the matrices of mass, damping and stiffness of the beam structure,  $R$  and  $R'$  and  $R''$  are the displacement, velocity and acceleration vectors, respectively.  $H_b P$  is equal to force vector on the node which comes from the interaction of the beam and the moving oscillator. By combining the Equations (7) of the beam and the moving oscillator, the vibration Equation (8) can be written as follows:

$$M(t)\ddot{Z} + C(t)\dot{Z} + K(t)Z = F(t) \tag{8}$$

$M(t)$ ,  $C(t)$  and  $K(t)$  are the matrices of time-varying vibration system of the beam and the moving oscillator and  $F(t)$  is the force vector, Equation (9).

$$\begin{aligned}
 M(t) &= \begin{bmatrix} M_b & 0 & H_b M_{V2} \\ 0 & M_{V1} & 0 \\ 0 & 0 & M_{V2} \end{bmatrix}; C(t) = \begin{bmatrix} C_b & H_b C_{V21} & H_b (C_{V22} - C_t) \\ 0 & C_{V11} & C_{V12} \\ C_t H_b^T & C_{V21} & C_{V22} \end{bmatrix}; \\
 K(t) &= \begin{bmatrix} K_b & H_b K_{V21} & H_b (K_{V22} - C_t) \\ 0 & K_{V11} & K_{V12} \\ K_t H_b^T + C_t H_b^T & K_{V21} & K_{V22} \end{bmatrix}; F(t) = \begin{bmatrix} H_b P_0 \\ 0 \\ 0 \\ C_{t1} r(\tilde{x}_1(t)) \tilde{x}_1(t) + K_{t1} r(\tilde{x}_1(t)) \\ C_{t2} r(\tilde{x}_2(t)) \tilde{x}_2(t) + K_{t2} r(\tilde{x}_2(t)) \end{bmatrix} \tag{9}
 \end{aligned}$$

$\ddot{Z}$ ,  $\dot{Z}$ ,  $Z$  are vectors of the displacement, velocity and acceleration of the beam vibrating system and the moving oscillator.

The Newmark- $\beta$  method is used to obtain dynamic response of the nodes in the beam due to the passing of the moving oscillator. Then acceleration-time history is obtained from the beam midpoint. The signals are then decomposed into the main modes using the EMD method, as explained in the next section.

### 2.3. Properties of beams and moving oscillator

A simply supported beam with a moving oscillator is used for this purpose. The beam is divided into 8 parts using the finite element method. Tables 1 and 2 shows geometric and physical properties of the beam and the moving oscillator.

Young's modulus	70 GPa
Cross-sectional area	200 mm <sup>2</sup>
Length of beam	820 mm
Moment of Inertia	$I_x = 1666.67 \text{ mm}^4$ $I_y = 6666.67 \text{ mm}^4$
Density	2700 kg/m <sup>3</sup>

Table 1. Properties of beams

$v = 2 \text{ m/s}$ ; $m_v = 0.5 \text{ kg}$ ; $m_1 = m_2 = 0.05 \text{ kg}$ ; $I_v = 0.0083 \text{ m}^4$ $s = 0.05 \text{ m}$ ; $a_1 = a_2 = 0.5 \text{ m}$ ; $K_{s1} = K_{s2} = 490.5 \text{ N/m}$ ; $K_{t1} = K_{t2} = 4900.5 \text{ N/m}$ $C_{s1} = C_{s2} = C_{t1} = C_{t2} = 0.2$ ; $l = 0.000167 \text{ m}^4$
--

Table 2. Properties of moving oscillator

### 3. EMD method

The EMD method is based on simple assumption that each signal consists of some fundamental components. According to this method, each signal can be decomposed into a number of signals that must satisfy the following conditions [16]:

- The number of the zero crossings and the extrema are equal or differ at most by one, and
- The average value of the local extrema and the minima of the envelopes is equal to zero.

These decomposed signals are called IMFs. In order to decompose the time domain signal and to gain IMFs, the following steps should be considered:

- Determining all local maxima and minima of the signal.
- Connecting the maxima points together using the cubic

spline interpolation technique and repeating the same procedure for the minima points.

- Calculating the mean value of the function lines corresponding to the maxima and the minima of  $m_1$  and related difference with the value of the main input signal related to the vibrations  $x(t)$ , which is set to  $h_1$  [16].

$$x(t) - m_1 = h_1 \quad (10)$$

where  $h_1$  is the first member to be checked for IMF requirements. For this purpose, two above IMF conditions must be considered. If it is supposed as an IMF,  $h_1$  is separated from the original signal as of the first IMF and is called  $c_1$ . The residue is called  $r_1$ . Through the next step,  $r_1$  is treated just like the original signal and the above process is repeated [16].

$$r_1 = x(t) - c_1 \quad (11)$$

$$r_{n-1} - c_n = r_n \quad (12)$$

If  $h_1$  is not an IMF, it should be treated as the original signal and the same steps (1 to 3) need to be iterated. The iteration continues till  $k$ -steps to make sure that is an IMF.

$$h_1 - m_{11} = h_{11} \quad (13)$$

$$c_1 = h_{1k} \quad (14)$$

This process of decomposition is supposed to be completed when the last residue  $r_n$  has at most one local extremum [16].

$$sd = \sum_f \left[ \frac{|h_{n-1}(t) - h_n(t)|^2}{h_{n-1}^2(t)} \right] < \varepsilon \quad (15)$$

where  $n$  is the steps of the process and  $\varepsilon$  is considered to be between 0.2 and 0.3. If the function  $r$  satisfies the previously mentioned conditions, the algorithm stops, otherwise, the previous steps should be repeated. As the decomposition steps are passed, the main signal can be represented as follows [17-19].

#### 4. Short-time fourier transform (STFT)

In dealing with non-stationary signals, it can be assumed that there are some stationary components. If the stationary part of the signal is too small, appropriate small size windows should be used. In this method, the signal is divided into small enough components that are supposed to be stationary. For this purpose, a step is chosen in which the width of the step is equal to the part of the signal that its stationary assumption is variable. This step is initially

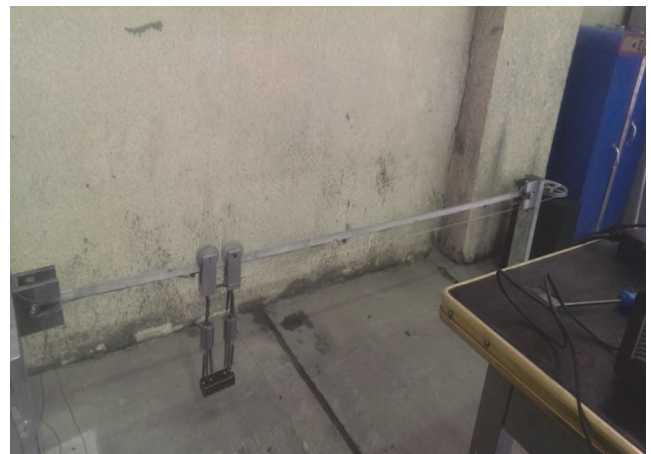
placed at the beginning of the signal  $t = 0$ . Assuming the step width as  $T$  seconds, at time  $t = 0$ , the step will cover the first  $T/2$ s of the signal. In the next step, a step is multiplied by the signal. If the step is supposed to be a rectangle with a value of 1, the product will be equal to the same part of the signal. This product is then processed as an independent signal by Fourier transform.

$$STFT_f^{(w)}(t, w) = \int [f(t) \times w^*(t - t')] \times e^{-iwt} dt \quad (16)$$

where  $f(t)$  is the signal,  $w(t)$  is a window function (step), and  $*$  is the sign of complex conjugate of the function. If the signal separated from the main signal is stationary, its Fourier spectrum can be considered as an accurate representation of the frequency content of the first  $T/2$  s of the signal. Then the step needs to move into the next part of the signal and the same procedure repeats. This process continues until the end of the signal.

#### 5. Beam and moving load modelling

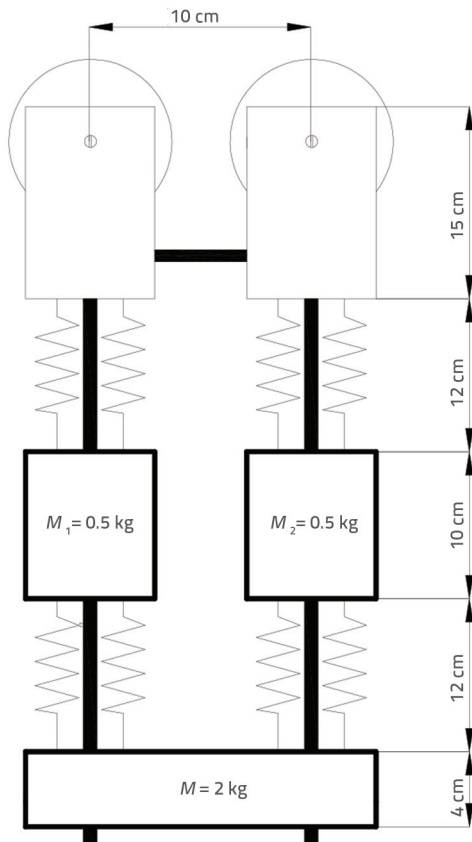
An aluminium beam 2 m in length and 20×10 mm in cross section is tested experimentally. Both ends of the beam are attached to two half-meter columns as shown in Figure 2. The self-weight of the aluminium beam and any applied loads are entered into the ball bearings at both ends which precisely have the same behaviour of simple joint support. A reverse vehicle is used to model the dynamic excitation system as



shown in Figures 3 and 4 in the laboratory and schematically, respectively.

Figure 3. Simple support

According to Figure 4, the proposed vehicle consists of two Teflon-type wheels to be in contact with the beam during the experiment due to its self-weight. Two 0.5 kg masses called  $m_1$  and  $m_2$ , connected to a 2 kg mass by using two tensile springs, are attached to the wheels. The vehicle is driven by an electric motor including a gearbox at a constant speed of 1m/s, causing



vibration in the beam. The shape and location of cracks are presented in Figure 5.

Figure 4. Physical model of moving load

### 6. Extraction of vibration signals

To extract vibrational signals of the beam, three B&K

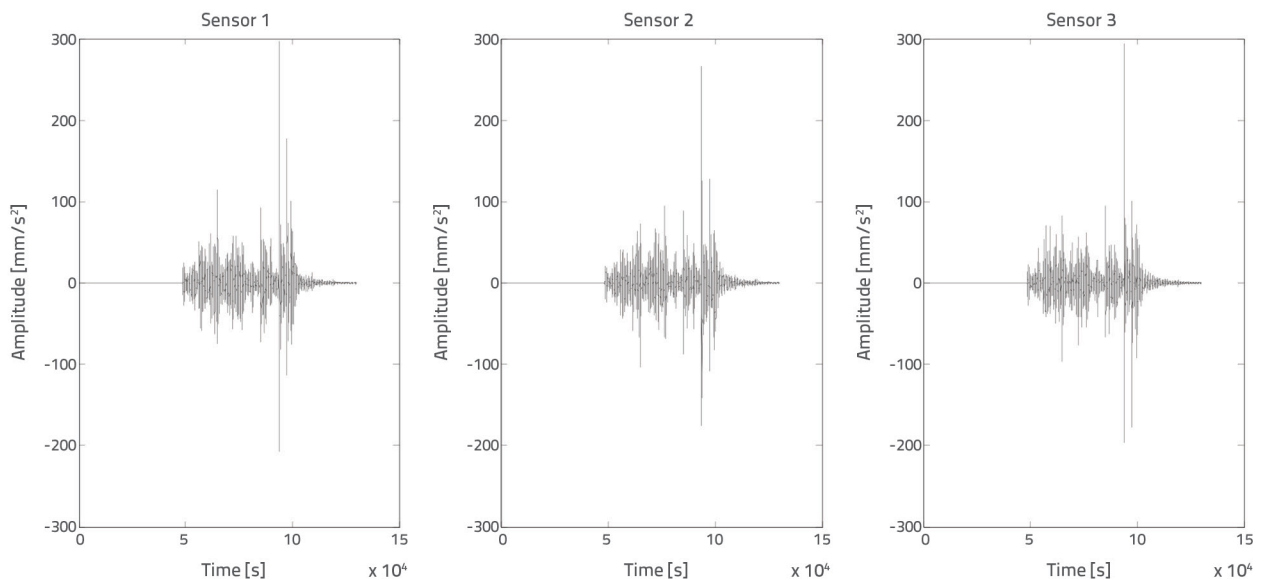


Figure 7. Acceleration time history for safe beam in first test

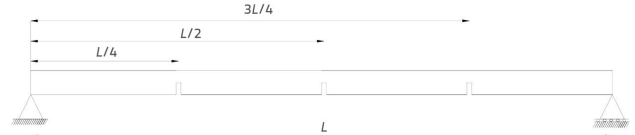


Figure 5. Location of crack in beam

Accelerometer Sensors (Type 4507) are installed at the upper part of the beam at 168, 94, 54 cm of the beam length. The test is implemented with a sampling frequency of 6.4 kHz, as the sensors have the capability of recording even the slightest vibrations. The vehicle is driven by an electric motor at a constant speed of 1m/s and passes the entire length of the beam to generate vibrations along the beam. The signals are stored by the accelerometers. To increase reliability, each test is repeated 20 times. On the other hand, during each test, the signals extracted from all three sensors at different locations are repeated twenty times, and so generally 60 signals are gained for each damage



scenarios. A scheme of the laboratory is shown in Figure 6.

Figure 6. Beam in laboratory

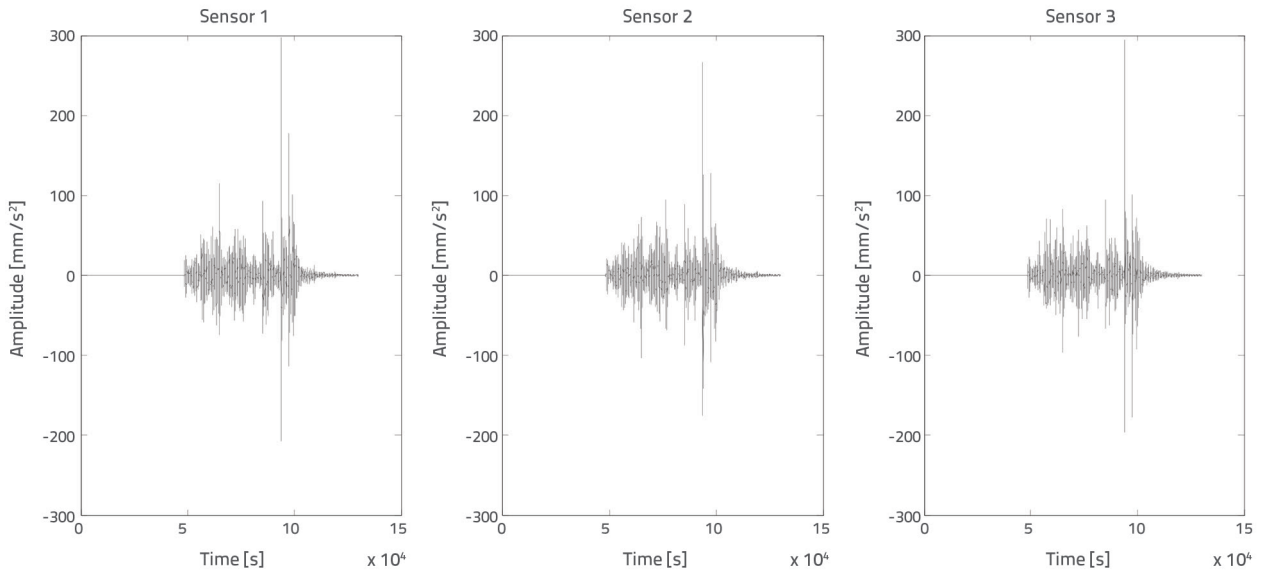


Figure 8. Acceleration time history for safe beam in second test

Three cracks, which are made by using low thickness saws, are placed on the beam at  $1/4$ ,  $1/2$  and  $3/4$  of the length of the beam with damage intensities of 50 % and 80 % (d/h). The test is repeated twenty times on each one of the cracks. In the first case, the intact beam is tested by moving the vehicle twenty times over the beam at a constant speed of 1 m/s, and the acceleration results are stored in each experiment separately. The vehicle passage results are shown in Figures 7 and 8 for the intact beam.

As shown in Figures 7 and 8, the beam oscillated as the vehicle began to move along the beam, and the oscillations diminished

with the passage of the vehicle to a non-vibrating state. By assessing the signals of the twenty experiments, it can be concluded that the system is reproducible. In the second case, the crack is placed at  $1/2$  of the length of the beam with 50 % and 80 % of damage and the same experimental procedure of the intact beam is repeated. The results of the test are stored for all twenty times of repetition distinctly. The results of the first two experiments with 50 % of damage intensity are shown in Figure 9. In the third and fourth cases, the cracks are placed at  $1/4$  and  $3/4$  of the length of the beam with 50 and 80 % of damage intensities. The same steps of vehicle passing are

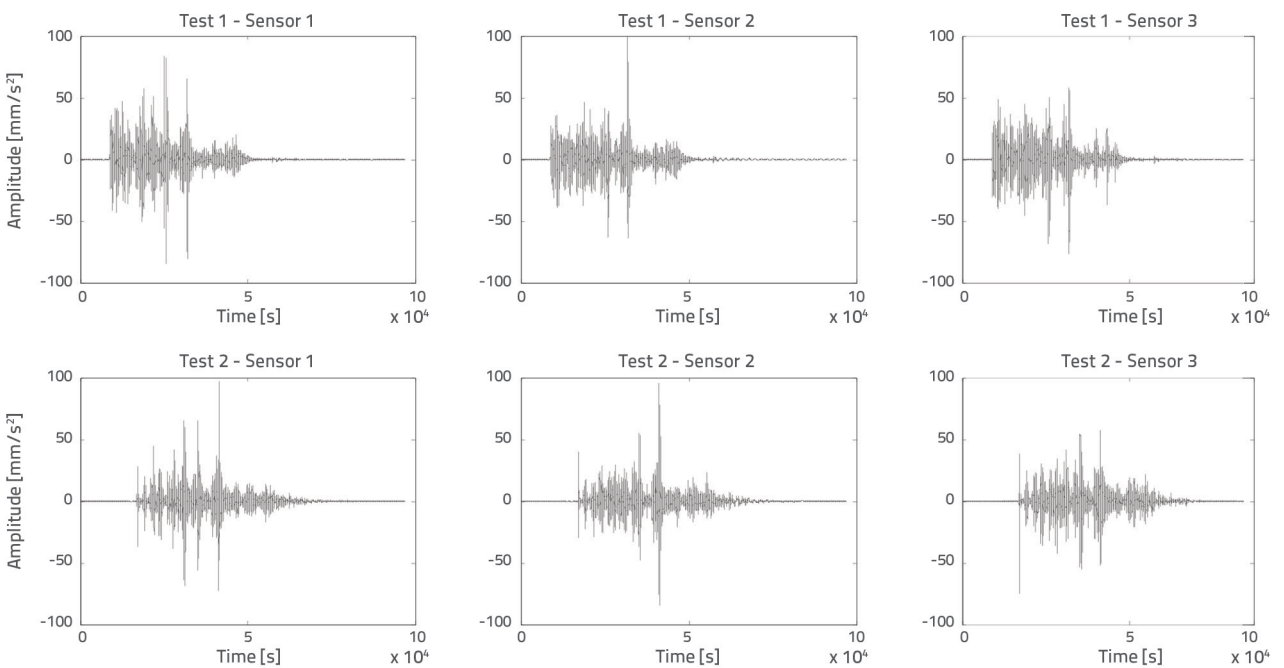
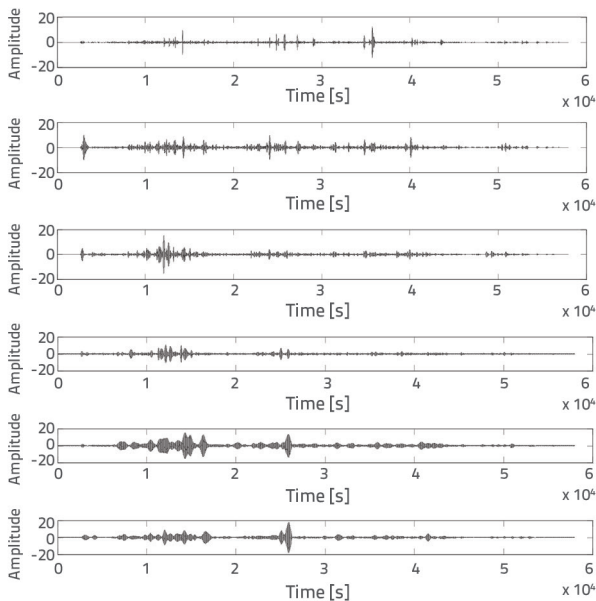


Figure 9. Acceleration time history for beam damage in first and second test

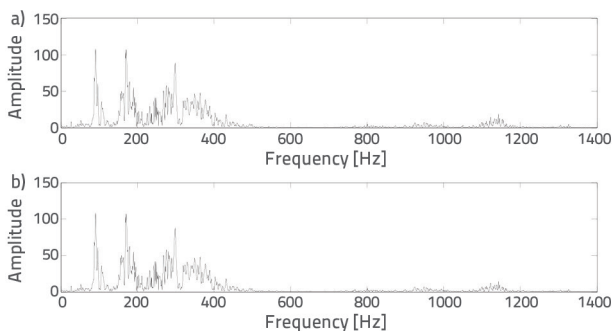
repeated over the beam and the results are stored separately. However, the results are not presented due to similarities. As illustrated in Figure 10, the acceleration signal obtained from the first experiment in the first sensor is converted to



31 frequency ranges, and only the first five components are presented in this figure.

**Figure 10.** IMFs extracted from acceleration time history signal

According to Figure 11, the sum of the frequency range and frequency of the main signal fit perfectly. The results of the EMD are converted to the frequency range using the short-time Fourier transform method and then the dominant frequencies of each IMF are obtained, and are used as features for the FGA. It should be noted that at this stage thirty-one IMFs are gained from each signal. Then the dominant frequency of each component is obtained by using the Fourier transform. On the other hand, three signals are gained per test, and each of them includes 31 dominant frequencies. Lastly, 1860 frequencies are

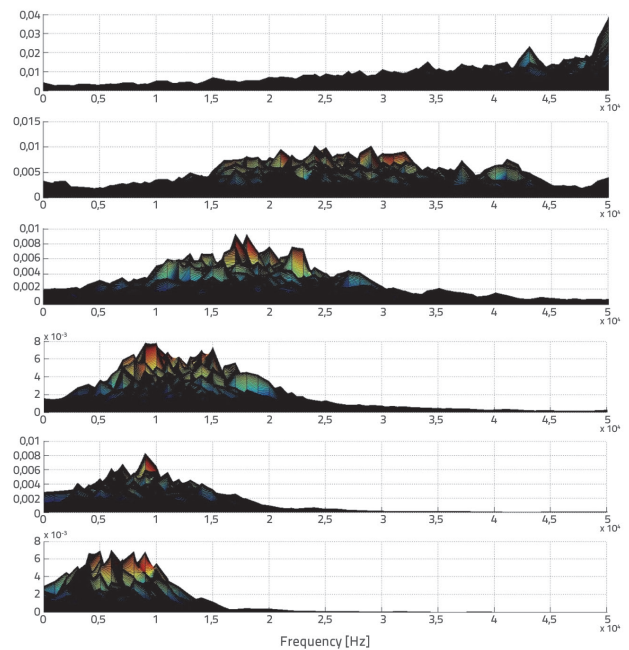


achieved by considering twenty repetitions in each case.

**Figure 11.** Compliance of two frequencies from sum of 31 IMFs: a) the frequency of EMD; b) the frequency of original signal

**with PSD**

Since this number of features is too high for the FGA, only 3 frequencies are extracted from each signal and, based on the current assumption, 9 frequencies are acquired. Also, as mentioned, the FGA must be trained and then verified after completing the test process and the percentage of the correct answers can be expressed. For this purpose, the first 10 tests are considered for algorithm training and the next 10 for the validation. The frequencies of the intact beam for the first experiment and the first sensor are illustrated in Figure 12 by using the short-time Fourier transform. It should be noted that the three-dimensional



time-frequency-value figures are presented as two-dimensional frequency-value plots in Figure 12.

**Figure 12.** STFT diagram of time-frequency value of intact beam for all IMFs in first test in sensor 1

## 7. Genetic-fuzzy algorithm

Based on the created membership functions, fuzzy logic (FL) is a high-capacity algorithm for the classification of data. Due to the FL requirement for the values of the mean and the standard deviation of data, which can be optimized by the GA, the combination of the FL and GA results in an efficient algorithm.

### 7.1. Damage indicator modelling

The damage indicator is considered as the difference between ninety dominant natural frequencies obtained from the short-time Fourier transform output for both intact and the damaged cases in the beam. This is defined in a non-dimensional form as follows:

$$\Delta\omega = \frac{\omega^{(u)} - \omega^{(d)}}{\omega^{(u)}} \quad (17)$$

where  $\Delta\omega$  is the frequency difference in non-dimensional form,  $\omega^{(u)}$  denotes the dominant natural frequency of the intact case, and  $\omega^{(d)}$  is the dominant natural frequency of the damaged case.

## 7.2. Damage detection system design

In this system, natural frequencies of each scenario are subtracted from the frequencies of the intact beam and then divided by the same intact case frequencies. The values are normalized between zero and one as listed in Table 3. Therefore, one intact and six damaged scenarios are defined. The fuzzy system input is taken as the normalized frequency difference, and the output is defined as the location and severity of damage. However, the main objective is to find the relationship between the inputs and the outputs. The first step in defining the fuzzy system is fuzzification of the existing data into a linguistic expression. For this purpose, each normalized frequency difference is converted into five sections as shown in Table 4. The next step is to define membership functions. A membership function is a function that is based on the input data, and a value

between zero and one is specified for the output. In this paper, Gaussian membership functions are used for input variables. This function can be defined as follows:

$$\mu(x) = e^{-0.5\left(\frac{x-m}{\delta}\right)^2} \quad (18)$$

where  $m$  is the midpoint of the fuzzy function and  $\delta$  is the standard deviation related to the variables. Gaussian fuzzy membership functions are very common in fuzzy systems. The midpoints for these functions must be chosen in such a way that the frequency range is covered appropriately.

The selection of standard deviation for fuzzy functions is highly important due to its great effects on the performance of the fuzzy system. A rule is specified to obtain the fuzzy rules by converting the numerical frequency difference into linguistic expressions at any location and severity of damage. Based on the membership function defined in the previous step, the degree of the membership associated with each frequency difference is gained.

Each frequency difference is assigned to a membership function with the maximum value. Following the above-mentioned process and considering the linguistic expressions defined in Table 2, seven rules are achieved as listed in Table 3. These rules

**Table 3. Normalized frequency difference between 0 and 1**

$\Delta\omega_{90}$	...	$\Delta\omega_2$	$\Delta\omega_1$	Intensity [%]	Damage location
0.05	...	0.15	0.49	50	in 50 cm
0.56	...	0.29	0.53	80	
0.67	...	0.34	0.45	50	in 100 cm
0.56	...	0.56	0.65	80	
0.09	...	0.87	0.98	50	in 150 cm
0.34	...	0.56	0.34	80	

**Table 4. Fuzzy-Gaussian functions to fuzzify numerical values**

0.87-1	0.62-0.87	0.37-0.62	0.12-0.37	0-0.12
Very high (VH)	High (H)	Moderate (M)	Low (L)	Very low (VL)

**Table 5. Fuzzy system rules**

$\Delta\omega_{90}$	...	$\Delta\omega_2$	$\Delta\omega_1$	Severity of the damage [%]	Damage location
N	...	N	N	Safe	Safe
VL	...	L	M	50	in 50 cm
M	...	L	M	80	
H	...	L	M	50	in 100 cm
M	...	M	H	80	
VL	...	H	VH	50	in 150 cm
L	...	M	L	80	

can be interpreted for specific cases as follows:

If M, L, and VL are the first frequency difference, the second frequency difference, and the frequency difference of 90, respectively, the intensity of the damage in 50 cm of the length of the beam is equal to 50 %.

The rules related to other damage cases can be interpreted in the same way. As listed in Table 3, each rule has a unique effect which is completely different from other rules. Therefore, the defined fuzzy system can be considered as a good classifier. These rules generate basic knowledge and show how an expert uses the interpretation of frequency changes for damage detection.

After rules definition, the GA, which is highly different from traditional methods, is used for the optimization of membership functions. In this algorithm, the design space must be converted into a genetic space. Therefore, GA works with a set of coded variables. This algorithm is used in this manuscript to find the midpoints and the standard deviation of the specified fuzzy Gaussian functions. For this purpose, the cost function must first be defined for finding the minimum. The objective function is defined and described as follows:

$$FF = \frac{\sum_{i=1}^{27} \sum_{j=1}^9 (\alpha_{ij} - \beta_{ij})^2}{27 \times 9} \tag{19}$$

where  $\alpha$  is the optimal output value of the fuzzy system and  $\beta$  is the actual output value of the fuzzy system. The optimal output is assumed in such a way that if the fuzzy system data is applied to a damage case, the related rule of the mentioned damage outputs the value one, and the other rules are taken as zero.

To produce the next generation based on the values obtained from the objective function, the best population of the present generation is copied at the rate of one. However, genetic parts of the algorithm should be used to produce the rest of the population. The crossover operator, which is used to combine the genetic information of two parents to generate new offspring, consists of three operations:

- a pair of strings are selected randomly

- a crossover point is chosen over the string
  - finally in the third step the offspring are created by exchanging the strings values based on the crossover point.
- In this manuscript, the rate is set to 8 to produce the child. Another operator in the GA is the mutation operator that is a random modification of a child through the population in which the rate of this operator is chosen as 2 in this paper. Therefore, the optimum value for the fuzzy midpoints and the standard deviation are gained after 100 iterations with the objective function value of 0.69.

For reliability assessment of the designed fuzzy system, the frequency difference values are utilized to define the system's inputs. Also, to gain the fuzzy system output, the midpoint of fuzzy sets corresponding to the 90 frequency difference outputs is used as the fuzzy system output represented in Table 6. As per Table 6, the fuzzy system can produce the maximum value of one in each damage case. It means that the designed system meets the preliminary requirement for predicting the damage's respective location and severity.

After the training stage, implemented and validated by the first ten experiments, the proposed method is applied for ten further tests not included in the training phase. The most significant point is that all signals in this stage are contaminated with noise to satisfy the real-world noisy signals condition. Similarly, the extracted properties, parameters and class numbers from the tests are considered the fuzzy system's input and output, respectively. By comparing this class number with the correct class number in each simulation, the success rate  $S_R$  can be calculated as follows:

$$S_R = \left( \frac{N_C}{N} \right) \times 100 \tag{20}$$

where N is the total number of the simulated samples and  $N_C$  is the number of the correctly detected samples in the corresponding class in Table 5. The value of the success rate for each damage case and the average success rate value are also listed in Table 5. In order to study the effect of the measured noise, different noise percentages are applied to the extracted features, and then the success rate value is presented for

**Table 6. Output of fuzzy rules with different frequency data**

Output of Rules 7	Output of Rules 6	Output of Rules 5	Output of Rules 4	Output of Rules 3	Output of Rules 2	Output of Rules 1	Severity of the damage	Damage location
0.32	0.97	0.08	0.63	0.76	0.34	1	Safe	Safe
0.16	0.21	0.76	0.13	0.54	1	0.34	50 %	Damage in 50 cm
0.26	0.28	0.21	0.11	1	0.32	0.34	80 %	
0.43	0.06	0.11	1	0.42	0.41	0.25	50 %	Damage in 100 cm
0.32	0.08	1	0.42	0.27	0.42	0.31	80 %	
0.14	1	0.31	0.59	0.44	0.54	0.13	50 %	Damage in 150 cm
1	0.19	0.23	0.60	0.54	0.68	0.12	80 %	

each class. Obviously, noise can cause errors in the measured data. Although the use of modern equipment has reduced the noise, it can never be eliminated. Therefore, the fault detection system should not only work based on the ideal values but should also be capable of working in the presence of noisy data. In this study, uncertainties in modelling and measurement of noise are added to the frequency difference values. Equation 12 is defined for this purpose in which the random number  $u$  is selected in the range of  $\{-1,1\}$  and  $\alpha$  denotes the noise level [19]:

$$\Delta\omega_{\text{noisy}} = \Delta\omega + \alpha u \quad (21)$$

The  $\alpha$  parameter specifies the maximum variance between the value of  $\Delta\omega$  and the simulated value of  $\Delta\omega_{\text{noisy}}$ . For instance, if  $\alpha = 0.1$ , the value of  $\Delta\omega_{\text{noisy}}$  can differ from the  $\Delta\omega$  value by ten percent. Therefore,  $\alpha$  is used to control the noise level in the fuzzy system input data.

To assess performance of the damage detection system for each noise level, the noise is added into the frequency data of the beam by using Equation (12). Then the noise data is applied to the fuzzy system and the accuracy of the damage detection results is calculated. The rate of the correct results based on

$\alpha = 0.3$	$\alpha = 0.2$	$\alpha = 0.1$	$\alpha = 0.05$	Rule
81.9	88.3	91.2	98.3	1
76.4	81.3	89.4	99.3	2
70.3	74.3	81.3	97.4	3
69.9	76.6	85.5	98.5	4
71.1	86.6	90.4	96.8	5
61.2	71.2	88.4	92.5	6

## REFERENCES

- [1] Lotffolahi-Yaghin, M.A., Koohdaragh, M.: Examining the function of wavelet packet transform (WPT) and continues wavelet transform (CWT) in recognizing the crack specification. *KSCSE Journal of Civil Engineering*, 15 (2011) 3, pp. 497–506, doi: 10.1007/s12205-011-0925-2
- [2] Araki, Y., Miyagi, Y.: Mixed integer nonlinear least-squares problem for damage detection in truss structures, *Journal of Engineering Mechanics*, 131 (2005) 7, pp. 659–667, doi: 10.1061/(ASCE)0733-9399(2005)131:7(659)
- [3] Ge, M., Lui, E.: Structural damage identification using system dynamic properties, *Computers & Structures*, 83 (2005) 27, pp. 2185–2196, doi: 10.1016/j.compstruc.2005.05.002
- [4] Jiang, L., Wang, K.: An enhanced frequency-shift-based damage identification method using tunable piezoelectric transducer circuitry, *Smart Materials and Structures*, 15 (2006) 3, pp. 799–808, doi: 10.1088/0964-1726/15/3/016
- [5] Lu, Z.R., Liu, J.K., Huang, M., Xu, W.H.: Identification of local damages in coupled beam systems from measured dynamic responses, *Journal of Sound and Vibration*, 326 (2009) 2, pp. 177–189, doi: 10.1016/j.jsv.2009.04.028
- [6] Lina Ding, Z., Hong Hao, R., Xinqun Zhu, I.: Evaluation of dynamic vehicle axle loads on bridges with different surface conditions, *Journal of Sound and Vibration*, 323 (2009) 4, pp. 826–848, doi: 10.1016/j.jsv.2009.01.051

different levels of noise is listed in Table 5.

### Table 7. Amount of success rate ( $S_R$ )

According to Table 7, at 0.05 of noise level, the damage detection is performed efficiently in all damage classes and is significantly successful. As the noise increases, as expected, the capability of the proposed method to successfully detect the damage classes is reduced, but it is still possible to identify the damage, which demonstrates the efficiency and high capability of the proposed methodology.

Table 7 shows the results from the second set of ten tests, including different noise levels. The results of the top rows of the table indicate the accuracy and robustness of the proposed technique.

## 8. Conclusion

In this study, a new portable intelligent mechanical system is introduced to detect damage in a beam structure by using the FGA. The proposed method is capable of detecting the location and severity of the damage. To obtain the features of the signals, the EMD method is used to decompose the acceleration-time history into its main components, each with a specific frequency range. Then, the short-time Fourier transform is utilized to extract the dominant frequency of each IMF as a feature for the FGA. The damage detection system is capable of detecting the location and severity of damage in all different scenarios, which is one of the advantages of the current study over previous researches. The following is suggested for prospective studies:

- Using a more extensive moving load system (mass and spring) with a higher degree of freedom increases the accuracy of modelling and, thus, a more accurate study of the system's dynamic response can be implemented.
- Further innovative methods may be used to extract natural frequencies from the acceleration diagram for a more detailed study of this vibrational system.

- [7] ean-Charles Wyss, H.O., Di Su, J., Yozo Fujino, T.: Prediction of vehicle-induced local responses and application to a skewed girder bridge, *Engineering Structures*, 3 (2011) 1, pp. 1088–1097, doi: 10.1016/j.engstruct.2010.12.020
- [8] Wu, S.Q., Law, S.S.: Vehicle axle load identification on bridge deck with irregular road surface profile, *Engineering Structures*, 33 (2011) 3, pp. 591–601, 2011.doi: 10.1016/j.engstruct.2010.11.017
- [9] Neves, S.G.M., Azevedo, A.F.M., Calçada, R.: A direct method for analyzing the vertical vehicle–structure interaction, *Engineering Structures*, 34 (2012) 12, pp. 414–420, Doi: 10.1016/j.engstruct.2011.10.010
- [10] Wu, S.Q., Law, S.S.: Evaluating the response statistics of an uncertain bridge–vehicle system, *Mechanical Systems and Signal Processing*, 27 (2012) 11, pp. 576–589, doi: 10.1016/j.ymsp.2011.07.019
- [11] Na, C., Kim, S., Kwak, H.: Structural damage evaluation using genetic algorithm, *Journal of Sound and Vibration*, 330 (2011) 12, pp. 2772–2783, doi: 10.1016/j.jsv.2011.01.007
- [12] Marano, G., Quaranta, G., Monti, G.: Modified genetic algorithm for the dynamic identification of structural systems using incomplete measurements, *Computer-Aided Civil and Infrastructure Engineering*, 26 (2011) 2, pp. 92–110, doi: 10.1111/j.1467-8667.2010.00659.x
- [13] Mosquera, V., Smyth, A., Betti, R.: Rapid evaluation and damage assessment of instrumented highway bridges, *Earthquake Engineering and Structural Dynamics*, 41 (2012) 4, pp. 755–774, doi: 10.1002/eqe.1155
- [14] Loh, C., Mao, C., Huang, J., Pan, T.: System identification and damage evaluation of degrading hysteresis of reinforced concrete frames, *Earthquake Engineering and Structural Dynamics*, 40 (2010) 6, pp. 623–640, doi: 10.1002/eqe.1051
- [15] Ganguli, R.: A fuzzy logic system for ground based structural health monitoring of a helicopter rotor using modal data, *Journal of Intelligent Material Systems and Structures*, 12 (2001) 6, pp. 397–407, doi: 10.1106/104538902022598
- [16] Xianfeng, F., Mingzuo, J.: Gearbox fault detection using empirical mode decomposition, *ASME International Mechanical Congress and Exposition*, 12 (2004) 4, pp. 456–467, doi: 10.1016/j.ymsp.2005.02.003
- [17] Dejie, Y., Junsheng, Z., Cheng, Y., Yang Y.: Application of EMD method and Hilbert Spectrum to the fault diagnosis of roller bearings, *Mechanical System and Signal Processing*, 19 (2003) 3, pp. 259–270, doi: 10.1016/S0888-3270(03)00099-2
- [18] Huang, N.E.: The empirical mode decomposition and Hilbert spectrum for nonlinear and non-stationary time series analysis, *Proceedings of the Royal Society A*, 454 (2002) 5, pp. 903–995, doi: 10.1098/rspa.1998.0193
- [19] Beena, P., Gangul, R.: Structural damage detection using fuzzy cognitive maps and Hebbian learning, *Journal of Applied Soft Computing*, 12 (2010) 3, pp. 132–144, doi: 10.1016/j.asoc.2010.01.023